Environ. Sci. Technol. **1999**, *33,* 2793−2799

Geochemistry of a Permeable Reactive Barrier for Metals and Acid Mine Drainage

S. G. BENNER,*,† D. W. BLOWES,† W. D. GOULD,‡ R. B. HERBERT, JR.,†,§ AND C. J. PTACEK†

Department of Earth Sciences, University of Waterloo, Waterloo, Ontario, N2L 3G1 Canada, and CANMET, Natural Resources Canada, Ottawa, Ontario, K1A 0G1 Canada

A permeable reactive barrier, designed to remove metals and generate alkalinity by promoting sulfate reduction and metal sulfide precipitation, was installed in August 1995 into an aquifer containing effluent from mine tailings. Passage of groundwater through the barrier results in striking improvement in water quality. Dramatic changes in concentrations of SO_4 (decrease of 2000−3000 mg/L), Fe (decrease of 270−1300 mg/L), trace metals (e.g., Ni decreases 30 mg/L), and alkalinity (increase of 800−2700 mg/L) are observed. Populations of sulfate reducing bacteria are 10 000 times greater, and bacterial activity, as measured by dehydrogenase activity, is 10 times higher within the barrier compared to the up-gradient aquifer. Dissolved sulfide concentrations increase by 0.2−120 mg/L, and the isotope ^{34}S is enriched relative to ^{32}S in the dissolved phase SO_4^{2-} within the barrier. Water chemistry, coupled with geochemical speciation modeling, indicates the pore water in the barrier becomes supersaturated with respect to amorphous Fe sulfide. Solid phase analysis of the reactive mixture indicates the accumulation of Fe monosulfide precipitates. Shifts in the saturation states of carbonate, sulfate, and sulfide minerals and most of the observed changes in water chemistry in the barrier and down-gradient aquifer can be attributed, either directly or indirectly, to bacterially mediated sulfate reduction.

Introduction

Discharge of acidic effluent, often containing high concentrations of toxic trace metals, from mines and mine waste is an intractable, worldwide environmental problem with estimated costs of treatment in the tens of billions of dollars. The oxidation of residual sulfide minerals in mines and mine waste can produce acidic waters containing high concentrations of sulfate, Fe(II), and trace metals. The oxidation of iron sulfide can be expressed as

$$2FeS_{2(s)} + 7O_2 + 2H_2O \Rightarrow 4SO_4^{2-} + 2Fe^{2+} + 4H^+$$

This effluent often enters underlying and adjacent aquifers where buffering by mineral dissolution raises the pH to 4−7 *(1)*. However, on discharge to the surface, the oxidation of Fe(II) to Fe(III) and the precipitation of ferric oxyhydroxides can regenerate acidic conditions (pH < 3):

$$4Fe^{2+} + O_2 + 10H_2O \Rightarrow 4Fe(OH)_{3(s)} + 8H^+$$

This generated acidity can mobilize toxic trace metals and adversely impact surface water ecosystems. Discharge from mines and mine waste can continue for decades, even centuries *(2)*. Conventional treatment by lime neutralization produces large volumes of metal-rich sludge and often involves long-term operating costs.

Sulfate reduction and metal sulfide precipitation have the potential to remediate acid mine drainage (*3*, *4*). In natural settings, sulfate reduction is mediated by sulfate reducing bacteria (SRB). Sulfate reducing bacteria are phylogenetically diverse and utilize a variety of biochemical pathways to reduce sulfate by oxidation of organic carbon. Sulfate reducing bacteria utilize short chain organic carbon compounds or H_2 to reduce SO_4 and are often dependent on a consortium of microorganisms to provide these substrates (*5*). A simplified expression of the reduction of sulfate by lactate can be expressed as

$$2CH_3CHOHCOO^- + 3SO_4^{2-} + 2H^+ \Rightarrow 6HCO_3^- + 3H_2S$$

The reduction of SO_4 and the production of dissolved sulfide species in the presence of dissolved metals can result in precipitation of metal sulfide mineral phases:

$$H_2S + Fe^{2+} \Rightarrow FeS + 2H^+$$

Other potential contaminants, including As, Cd, Cu, Fe, Ni, Pb, and Zn, can also react with sulfide to form sparingly soluble sulfide minerals. However, acidic waters can consume generated alkalinity and limit the ability of SRB to promote this reaction sequence (*6*). This limitation has hampered attempts to utilize sulfate reduction to treat acidic surface water associated with mine drainage (*7*, *8*). We have overcome this obstacle by promoting sulfate reduction within the aquifer, prior to increased acidification of the effluent upon discharge to the surface. Treatment within the aquifer is accomplished using a passive in situ permeable reactive barrier composed of organic material *(9)*. The organic carbon promotes sulfate reduction and metal sulfide precipitation as the contaminated groundwater flows through the structure.

The reactive barrier, containing a mixture of municipal compost (20 vol %), leaf mulch (20%), wood chips (9%), gravel (50%), and limestone (1%), was keyed to underlying bedrock at the base and outcropping bedrock at the sides. The installed barrier extends 20 m across the aquifer and is 3.5 m deep, and the barrier is 4 m thick in the direction of flow. Zones of sand, approximately 1 m thick, were also installed at the up- and down-gradient sides of the organic carbon mixture. These sand zones square off the barrier with the sloping sides of the trench, help to redistribute flow, and facilitate uniform sampling. A protective clay cap (30 cm) was placed over the barrier to minimize oxygen diffusion and flow of infiltrating water into the barrier. The barrier installation is described in detail in Benner et al. *(10)*. This barrier is the first full-scale reactive barrier in the world designed to treat metals and acid mine drainage using reductive processes. The installation provides a unique opportunity to evaluate, under controlled conditions, changes in groundwater

* Corresponding author phone: (519)888-4567 ext. 3438; fax: (519)746-3882; e-mail: sgbenner@scimail.uwaterloo.ca.
† University of Waterloo.
‡ CANMET, Natural Resources Canada.
§ Present address: Department of Geology and Geochemistry, Stockholm University, S-106 91 Stockholm, Sweden.

10.1021/es981040u CCC: $18.00
Published on Web 07/13/1999

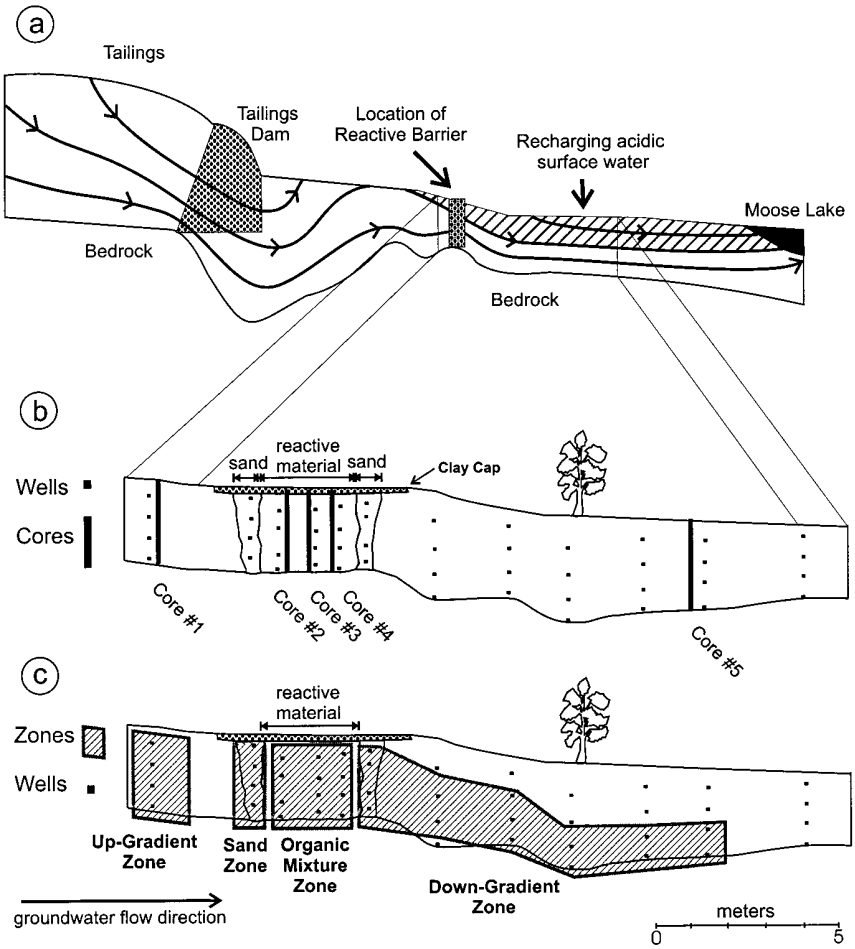

FIGURE 1. Cross-sectional profiles of aquifer and reactive barrier: (a) shows flow lines for the Nickel Rim aquifer prior to the installation of the reactive barrier determined by field-collected data and flow modeling from Bain (2000), (b) sample well and core locations in aquifer and reactive barrier, and (c) location of geochemically distinct zones along groundwater flow path.

geochemistry. Though the barrier is an engineered system, geochemical changes closely match processes associated with sulfate reduction in natural settings such as sediments and aquifers. This paper describes geochemical, microbiological, and mineralogical processes occurring within the permeable reactive barrier and adjoining aquifer.

Site Description. A groundwater plume, containing high concentrations of SO_4 (1000−5000 mg/L) and Fe (200−2000 mg/L) and a pH of 4−6, flows from the inactive Nickel Rim tailings impoundment into an adjoining alluvial aquifer (*11*−*13*). At the site of the installation, acidic surface water is recharging the aquifer. Figure 1(a) shows the flow field for the Nickel Rim aquifer prior to the reactive barrier installation (*10*−*12*). The aquifer receives water that has entered the aquifer through the tailings impoundment as well as acidic water infiltrating directly from the surface above the aquifer. This flow regime results in water entering the barrier from two distinct sources. The protective clay cap prevents infiltration directly into the barrier, but acidic surface water continues to enter the aquifer on both the up- and down-gradient sides. Treated water exiting the down-gradient side of the barrier occupies only the lower half of the aquifer, whereas the upper half of the aquifer contains acidic water which has not undergone treatment. Groundwater velocity is approximately 15 m/a (*10*).

Methods

Water Sampling and Analysis. Monitoring wells were installed in nests along a transect roughly parallel to groundwater flow (Figure 1). Samples of groundwater were collected in September 1995, June and September 1996, and July 1997 (1, 9, 12, and 22 months after installation). A detailed description of well installation, water sampling, and field and laboratory analysis can be found in Benner et al. (*10*). Additional analyses include dissolved organic carbon by combustion and infrared detection (*14*) and sulfur isotope determination by thermal decomposition of barium sulfate and analysis on a mass spectrometer (*15*).

Solid-Phase Methods. Samples were collected using a 5 cm diameter driven coring device. Cores were collected in September 1996 for solid phase and mineralogical analysis and in September 1997 for bacterial analysis (Figure 1b). Cores, collected in aluminum casing, were sealed with plastic caps and refrigerated until analyzed.

The sulfate reducing bacteria were grown in a modified Postgate medium C in 20 mL serum bottles (*16*). The medium had the following composition in g/L: KH_2PO_4, 0.5; NH_4Cl, 1.0; Na_2SO_4, 4.5; $CaCl_2 \cdot 2H_2O$, 0.04; $MgSO_4 \cdot 7H_2O$, 0.06; Na lactate (60%), 2.92; Na acetate, 1.28; yeast extract, 1.0; $FeSO_4 \cdot 7H_2O$, 0.004; Na citrate$\cdot 2H_2O$, 0.3; and resaurzurin, 0.005 (pH adjusted to 7.5 using NaOH). Serum bottles containing medium were autoclaved, and 1 g sediment was added to each of five replicates. Inoculated samples were sequentially diluted and incubated in an anaerobic glovebox for 30 days. Positive growth of SRB was indicated by precipitation of Fe-sulfides. Values are reported as most probable number (MPN) determinations (*17*). Triphenyl tetrazolium chloride is a substrate for a number of nonspecific dehydrogenases

present in microflora and can be generally correlated with respiratory activity and used as an index of microbial activity (*18*). To determine dehydrogenase activity (DH), 5 g of sediment was buffered with $CaCO_3$ (to a pH > 6), and 1.75 mL of 0.5% 2,3,5-triphenyl tetrazolium chloride and distilled water were added. The samples were incubated for 24 h and extracted sequentially with two 10 mL aliquots of methanol and filtered through Whatman no. 42 paper. The aliquots were combined in a volumetric flask and made up to 50 mL with methanol. Optical density of the extract was measured at 485 μm. The enzyme activity assay was performed in triplicate and averaged.

Accumulations of monosulfides (operationally defined as acid volatile sulfides, AVS) and the AVS fraction plus disulfides and elemental sulfur (total reduced inorganic sulfur, TRS) were determined from core location no. 2 (Figure 1) within the organic mixture. The AVS and TRS extraction methods are described in detail in Herbert et al. (*19*) and involve the reaction of samples with cold 6 M HCl and hot chromous chloride solutions (*20*), respectively. Following reaction the evolved H_2S is trapped in a zinc acetate solution as ZnS and determined by iodimetric titration. A field emission scanning electron microscope employing energy-dispersive X-ray analysis (SEM-EDX) was used to obtain high-magnification images and elemental compositions of black accumulations on a sampling tube from within the permeable reactive barrier.

Geochemical Modeling. The geochemical speciation/mass transfer computer code MINTEQA2 (*21*), adjusted to be consistent with the WATEQ4F database (*22*), was used to aid in the interpretation of aqueous geochemical data. Input parameters were Al, Ca, Cl, Fe, K, Mg, Mn, Na, Ni, Si, SO_4, Zn, alkalinity, and pH. For water collected outside the reactive barrier installation, E_h was input from field platinum electrode measurements. Within the barrier, E_h was not specified, and measured concentrations of dissolved S^{2-} were input to calculate sulfide mineral saturation indices.

Results and Discussion

A striking improvement in water quality is observed after groundwater enters the reactive barrier. Concentrations of almost all measured dissolved species change (e.g. alkalinity increases 800−2700 mg/L, SO_4 decreases 2000−3000 mg/L, Fe decreases 270−1300 mg/L, and Ni decreases 30 mg/L; Figures 2 and 3). These changes indicate that significant geochemical transformations are occurring within the barrier.

Four Distinct Zones. For the purpose of evaluating geochemical, mineralogical, and microbiological changes attributed to the barrier, the aquifer can be viewed as being comprised of four zones. (Figure 1c). The up-gradient aquifer (up-gradient zone) contains mine-waste effluent water. This water first passes through the up-gradient sand fill (sand zone) and then the organic carbon mixture (organic mixture zone). Treated water flows into the lower portion of the down-gradient aquifer (down-gradient zone). Water chemistry analyses obtained during September 1996 from each vertical well nest along the flow path were averaged (Figure 3). Although these zones are chemically distinct, there is some variability from well point to well point within each zone (Figure 2).

Up-Gradient Zone. Bain et al. (*11, 12*) described the aquifer geochemistry prior to the reactive barrier installation. Geochemical analysis and modeling in this study are consistent with those results. The groundwater in the up-gradient zone is characterized by high concentrations of SO_4 (2500−5200 mg/L), Fe (250−1350 mg/L), and Ni (0.12−30 mg/L), pH between 2.8 and 5.9 and <1 to 60 mg/L alkalinity (as $CaCO_3$). The recharging acidic surface water (occupying the top meter of the up-gradient aquifer) contains higher concentrations of Al (130 mg/L), Ni (30 mg/L), Zn (1.0 mg/L), Cr (0.3 mg/L), and Cu (3.0 mg/L) and lower pH (<4).

Sulfate and Ca concentrations appear to be controlled by gypsum precipitation in the up-gradient zone (Figure 4). The groundwater is near saturated with respect to siderite ($FeCO_3$) in the lower portion of the aquifer and near saturated or supersaturated with respect to jarosite ($KFe_3(SO_4)_2(OH)_6$) or $Fe(OH)_3$ in the upper portion of the aquifer (*11*). Siderite dissolution has been proposed as a buffer to decreasing pH in this aquifer (*11*). Amorphous $Al(OH)_3$ probably controls aluminum concentrations. Silica concentrations range from 51 to 9 mg/L and appear to be limited by the solubility of amorphous SiO_2. No secondary mineral phase controls for Cl, Mg, Mn, Na, and Ni were identified. Other mechanisms such as coprecipitation or adsorption/desorption reactions with aquifer solids may limit concentrations of these species (*11*). Within the up-gradient zone, MPN for SRB average 2.3×10^2. Dehydrogenase activity (DH) values average 0.5 nmol h^{-1} g^{-1} (Figure 3).

Sand Zone. As water enters the sand zone, vertically averaged alkalinity increases to 150 mg/L, likely the result of calcite dissolution. MINTEQA2 calculations indicate slightly undersaturated conditions for calcite (Figure 4). Water entering the barrier is at equilibrium with gypsum. Calcium, released to the water by calcite dissolution, promotes gypsum precipitation. A corresponding decrease in SO_4 concentrations (to 3200 mg/L) is observed. Calcium concentrations, meanwhile, remain largely unchanged. Calcite dissolution coupled with gypsum precipitation commonly occurs in carbonate aquifers receiving acid mine drainage effluent (*11, 1*). Calcite dissolution may also produce the observed increase in pH. Though dissolved sulfide concentrations are low, it is also possible that sulfate reduction is occurring in the sand zone. Sulfate reduction can also explain the increase in alkalinity and pH and the decrease in SO_4 and Fe.

Geochemical calculations indicate near saturation with respect to amorphous $Al(OH)_3$. The precipitation of amorphous $Al(OH)_3$, driven by the increase in pH, likely explains the observed decreased Al concentrations (to <1.0 mg/L) (*23*). Within the sand zone, trace metal concentrations decrease to below analytical detection limits for Cu (<0.01 mg/L) and near detection levels for Zn (0.015 mg/L). Nickel concentrations decrease to 0.6 mg/L. Geochemical speciation calculations did not suggest precipitating mineral phases for these metals. High concentrations of trace metals originate from recharging acidic surface water. Declines in concentrations of these species may also be the result of reactions with aquifer sediment prior to entering the sand zone.

Organic Mixture Zone. As groundwater enters the organic mixture zone, average concentrations of SO_4^{2-} decrease 74% to 840 mg/L, while average alkalinity increases 1400% to 2300 mg/L, and S^{2-} increases 12 000% to 17 mg/L. Average populations of SRB (9.1×10^7) are 10^5 times greater, and DH (9 nmol $h^{-1}g^{-1}$) is 20 times greater than up-gradient zone values (Figure 3), indicating an elevated population of SRB is present and active within the barrier. Enrichment in ^{34}S in the remaining aqueous phase SO_4 (30‰ $\delta^{34}S$ compared to the up-gradient aquifer value of 5‰ $\delta^{34}S$) confirms that the observed decreases in SO_4 concentrations are due to bacterially mediated sulfate reduction (*24*). The large increase in alkalinity can be attributed to production of CO_2 by sulfate reducing and fermentative bacteria.

Elevated S^{2-} concentrations produce saturated to slightly supersaturated conditions for mackinawite ($Fe_{(1+x)}S$) and amorphous FeS (Figure 4). These phases commonly precipitate under sulfate reducing conditions in shallow ground and surface water systems (*25*). The results of solid-phase analysis indicate an accumulation of total reduced inorganic sulfur in the carbon mixture zone of up to 0.5 wt % S, compared with 0.025 wt % S in "unreacted" organic mixture

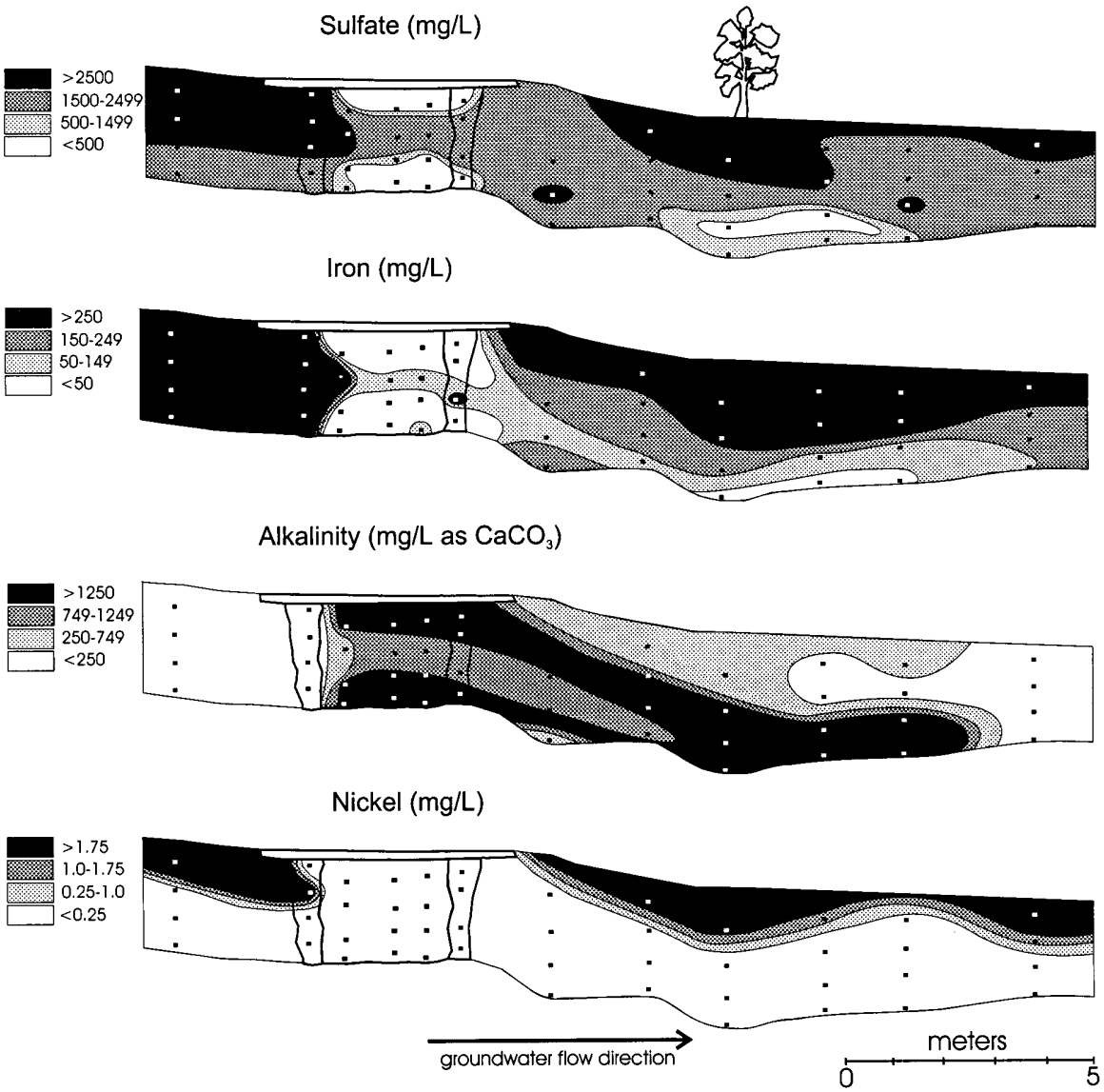

FIGURE 2. Cross-sectional profiles of dissolved constituents for September 1996: SO_4, Fe, alkalinity (as $CaCO_3$), and Ni.

(Figure 5). SEM-EDX analysis of black precipitates that accumulated on sampling tubes within the barrier indicate an Fe−S composition with a 1:1 stoichiometry, while X-ray defraction (XRD) analysis confirmed that the precipitates were poorly crystalline mackinawite ($Fe_{(1+x)}S$) (Figure 6) (*19*). The precipitation of these sulfide phases provides a sink for dissolved Fe which decreases >85% to an average of 80 mg/L. MINTEQA2 modeling indicates that the groundwater is near saturation with respect to siderite ($FeCO_3$) within the organic mixture zone. The precipitation of siderite may also contribute to the observed decrease in Fe concentrations.

Decreased SO_4 concentrations result in a shift from near equilibrium conditions for gypsum in the sand zone to undersaturated conditions in the organic mixture zone (Figure 4). Conversely, high alkalinity results in a shift in calcite stability from undersaturated in the sand zone to supersaturated conditions in the organic mixture zone. Increased alkalinity also results in supersaturation with respect to rhodochrosite ($MnCO_3$). Precipitation of rhodochrosite, or a less crystalline precursor, can explain the observed decrease in Mn concentrations. Mn may also be removed by coprecipitation with FeS or as a discrete manganese sulfide phase (*25*). The increase in pH to an average 6.7 versus 6.2 in the sand zone can be attributed to buffering between the carbonate and sulfide systems (*26*) and reflects the ability of this system to regulate pH conditions. Silica concentrations increase to an average value of 27 mg/L (Figure 3). This increase may be the result of enhanced silicate dissolution resulting from bacterial activity on silicate mineral surfaces (*27*) or may reflect increased Si solubility due to organic acid complexation (not accounted for by MINTEQA2 modeling) (*28*). Both of these mechanisms have been observed in organic-rich groundwater environments.

Concentrations of Ni decline to <0.1 mg/L within the organic mixture zone. MINTEQA2 calculations indicate slightly supersaturated conditions for millerite (NiS). Though Cu and Zn are present below detection within the organic mixture zone, geochemical calculations were made using analytical detection values. These calculations indicate that the pore water would be supersaturated with respect to the sulfide minerals chalcopyrite ($FeCuS_2$) and sphalerite (ZnS) suggesting a potential for these minerals, or less crystalline precursors, to precipitate. Laboratory studies have also shown effective removal of Ni, Cd, and Zn under sulfate reducing conditions (*29*). However, mechanisms removing trace metals from the water in natural anoxic sedimentary analogues are not well understood. Depending on geochemical conditions,

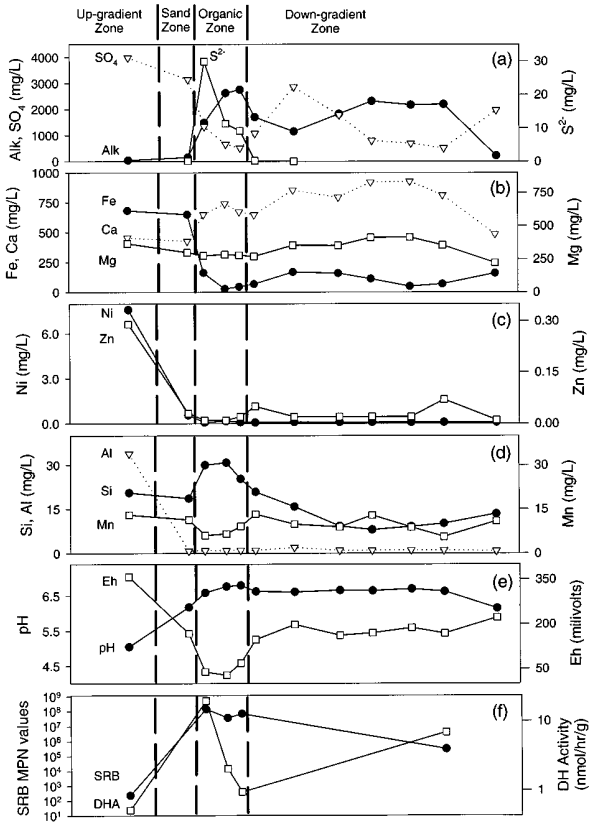

FIGURE 3. Vertically averaged constituent concentrations for each well nest: (a) SO_4, alkalinity (as $CaCO_3$), and S^{2-}, (b) Fe, Ca, and Mg, (c) Ni and Zn, (d) Si, Al, and Mn, (e) pH and E_h, and (f) vertically averaged most probable numbers (MPN) for sulfate reducing bacteria (SRB) and dehydrogenase enzyme activity (DH).

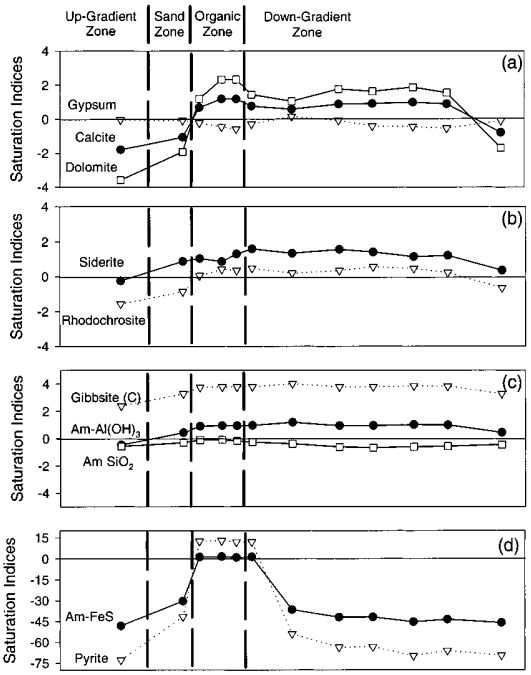

FIGURE 4. Vertically averaged saturation indices for selected mineral phases for each well nest: (a) gypsum ($CaSO_4 \cdot 2H_2O$), calcite ($CaCO_3$), and dolomite ($CaMg(CO_3)_2$), (b) siderite ($FeCO_3$) and rhodochrosite ($MnCO_3$), (c) gibbsite ($Al(OH)_3$), amorphous $Al(OH)_3$, and amorphous SiO_2, and (d) amorphous FeS and pyrite (FeS_2). Note: sulfide saturation indices outside organic material zone were calculated from measured E_h.

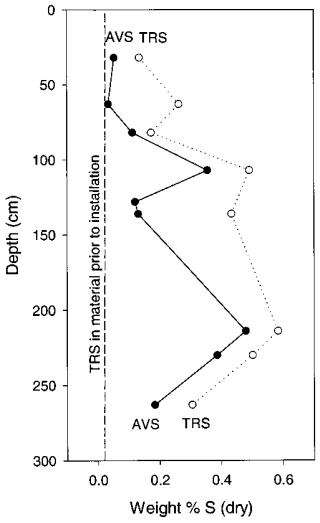

FIGURE 5. Vertical profiles of "acid volatile sulfide-AVS" and "total reduced (inorganic) sulfides-TRS" concentrations for organic material from core no. 2, September 1996. Dashed line indicates TRS concentration in organic material prior to installation of the barrier.

trace metals can adsorb, coprecipitate, or form discrete sulfide mineral phases under sulfate-reducing conditions (*6, 25*).

Barium concentrations increase from below analytical detection (<0.1 mg/L) in the up-gradient zone to 0.4 mg/L within the barrier. Geochemical calculations indicate that the water is locally undersaturated with respect to barite ($BaSO_4$). If present, barite may be dissolving within the barrier (*30*). Boron concentrations also increase from below analytical detection (<0.1 mg/L) to 0.6 mg/L. A solid-phase source for boron within the barrier was not identified. Phosphorus concentrations increase from below analytical detection 0.1 mg/L in the up-gradient zone to 5−20 mg/L in the organic material zone. The increase in P can be attributed to release from degradation of organic matter under anaerobic conditions (*23*).

Down-Gradient Zone. As the plume of treated water exits the permeable reactive barrier into the down-gradient aquifer, water chemistry again changes. Silica concentrations decrease to 13 mg/L. Depletion of dissolved organic carbon may eliminate enhanced silicate dissolution observed in the barrier. The S^{2-} concentrations decrease to an average 0.14 mg/L in the down-gradient zone. These S^{2-} concentrations are much lower (often less than the analytical level of detection, 0.05 mg/L) than within the organic mixture zone.

The absence of measurable S^{2-} concentrations precludes the direct determination of saturation indices for sulfide-bearing phases. Although sulfide speciation may be estimated using field-measured E_h values, it is unlikely that the state of the SO_4/S^{2-} couple is reflected in these measurements. However, evidence exists that sulfate reduction is occurring in the down-gradient aquifer. Black precipitates, similar in appearance to those identified as sulfides within the reactive barrier, were observed on well sampling tubes in the down-gradient zone. Dissolved organic carbon (DOC), a potential electron donor for sulfate reduction, is elevated in the down-gradient aquifer (50−200 mg/L). MPN values indicate populations of SRB (averaging 3×10^5) are 10^3 greater than in the up-gradient zone (Figure 3). Bacterial activity is also elevated with DH at 7 nmol h^{-1} g^{-1}. Geochemical modeling indicates that this water is supersaturated with respect to calcite, which is consistent with generation of alkalinity by SRB metabolic activity. Precipitation of sulfides may be

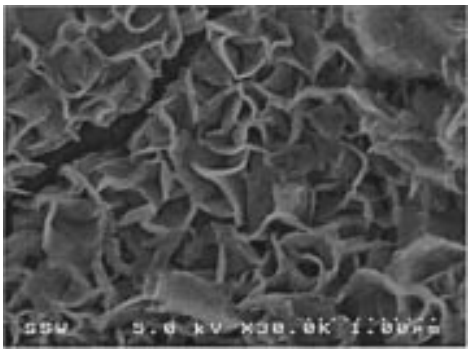

FIGURE 6. Scanning electron micrograph of black precipitates on sample tube within organic material zone identified by energy dispersive X-ray (EDX) as FeS.

occurring in reduced microenvironments associated with suspended or dissolved organic carbon. The most down-gradient sampling point in Figures 2 and 3 represents water that passed through the aquifer prior to the reactive barrier installation.

Vertical Trends within Barrier. Within the organic carbon zone, aqueous phase concentrations exhibit trends suggesting a greater degree of sulfate reduction at the top and bottom, compared to the middle, of the barrier. Concentrations of SO_4 are generally higher (>1500 mg/L) within the middle half than at the top and bottom of the barrier (<500 mg/L) (Figure 2). Iron shows a similar trend with values in the center >50 mg/L and generally <50 mg/L at the top and bottom. Conversely, alkalinity is generally <1250 mg/L in the central part of the barrier and >1250 mg/L at the top and bottom (Figure 2). Input water within the up-gradient sand zone does not exhibit these trends, suggesting they are the products of processes within the barrier.

Vertical stratification is likely caused by higher rates of flow through the middle portion of the organic mixture zone. Slower flow rates along the top and bottom of the barrier will result in longer residence times and may produce more complete reduction of sulfate, metal sulfide precipitation, and alkalinity generation. Shorter residence times through the middle of the barrier result in less SO_4 removed from a given pore volume. However, the higher flow rates through this zone may still produce higher rates of sulfide accumulation compared with slower zones above and below. Vertical profiles exhibiting higher accumulations of solid phase sulfides within the middle portion of the barrier are consistent with this conclusion (Figure 5). Most probable numbers for SRB and bacterial activity values do not exhibit obvious, clearly definable, trends within the reactive barrier. However, bacterial activity, as measured by dehydrogenase activity, and MPN values for SRB do suggest slightly higher bacterial populations are present in the middle of the barrier. These trends are consistent with trends in aqueous phase concentrations.

The permeable reactive barrier appears to be quite effective at maintaining E_h and pH conditions that support bacterially mediated sulfate reduction (5, *31*). The major changes in water chemistry and bacterial populations as groundwater passes through the barrier and the accumulation of solid phase sulfides within the barrier indicate that sulfate reduction and metal sulfide precipitation are the dominant mechanisms producing improved water quality. Nearly all observed changes in groundwater chemistry can be attributed, directly or indirectly, to these processes. Groundwater toxicity has been lowered in three significant ways: the generation of alkalinity, the elimination of acid generating potential, and the removal of trace metals. In addition, the precipitation of carbonate minerals within and down-gradient of the barrier results in the accumulation of solid-phase buffering capacity against the future influx of acidic groundwater. Lack of oxidizing agents within the groundwater, coupled with low mineral solubility, renders the accumulating sulfide phases within the barrier quite stable.

There is enough carbon within the barrier to treat the groundwater for hundreds of years; however, it is likely that only a fraction of the organic carbon is sufficiently reactive to promote rapid reduction of sulfate. Calculations, based on the long-term performance of column studies, indicate that the reactive barrier has a theoretical treatment lifetime of >15 years (*10*). However, direct transfer of these results from the laboratory neglects the potential complexities that exist in a field setting. Factors that may limit barrier performance in the field include preferential flow or preferential mass flux and low temperatures inhibiting bacterial activity. The long-term treatment capacity for the Nickel Rim reactive barrier will be determined by continued monitoring.

Acknowledgments

Funding for this research was provided by the Canadian Natural Sciences and Engineering Research Council (NSERC), Falconbridge Ltd. and the Ontario Centre for Research in Earth and Space Technology. The authors would like to thank Chris Hanton-Fong, Cheryl Sue, Lyne Lortic, Mike Moncur, and Scott Sale for their assistance with the laboratory and field work.

Literature Cited

(1) Morin, K. A.; Cherry, J. A. *J. Contam. Hydrol.* **1988**, *2*, 323.
(2) Dubrovsky, N. M.; Cherry, J. A.; Reardon, E. J. *Can. Geotech. J.* **1985**, *22*, 110.
(3) Wakao, N.; Takahashi, T.; Sakurai, Y.; Shiota, H. *J. Ferment. Technol.* **1979**, *57*, 445.
(4) Machemer, S. D.; Wildeman, T. R. *J. Contam. Hydrol.* **1992**, *9*, 115−131.
(5) Chapelle, F. H. *Groundwater Microbiology and Geochemistry*; John Wiley & Sons Inc.: New York, 1993; p 87.
(6) Hao, O. J.; Chen, J. M.; Huang, L.; Buglass, R. L. *Crit. Rev. Environ. Sci. Technol.* **1996**, *26*(1), 155−187.
(7) Dvorak, D. H.; Hedin, R. S.; Edenborn, H. M.; McIntire, P. E. *Biotech. Bioeng.* **1992**, *40*, 609−616.
(8) Bechard, G.; McCready, R. G. L.; Koren, D. W.; Rajan, S. *Proceedings of Sudbury '95- Mining and the Environment;* Sudbury, Ontario, May 28−June 1, 1995; pp 545−554.
(9) Blowes, D. W.; Ptacek, C. J. U.S. Patent no. 5514279, 1994.
(10) Benner, S. G.; Blowes, D. W.; Ptacek, C. J. *Ground Water Monit. Remed.* **1997**, *17*, 99−107.
(11) Bain, J. G.; Blowes, D. W.; Robertson, W. D. *Proceedings of Sudbury '95- Mining and the Environment* Sudbury Ontario, May 28−June 1, 1995, pp 715−723.
(12) Bain, J. G.; Blowes, D. W.; Robertson, W. D. *J. Contam. Hydrol.* **2000**, in press.
(13) Johnson, R. H.; Blowes, D. W.; Robertson, W. D.; Jambor, J. L. *J. Contam. Hydrol.* **1999**, in press.
(14) *Standard Methods for the Examination of Water and Wastewater*; APHA: Washington, DC, 1996; pp 5−11.
(15) Yanagisawa, F.; Sakai, H. *Anal. Chem.* **1983**, *55*, 985.
(16) Postgate, J. R. *The Sulphate-Reducing Bacteria*; Cambridge University Press: Cambridge, England, 1984.
(17) *Agronomy*; Alexander, M., Black, C. A., Eds.; 1965; Vol. 9, pp 1467−1472.
(18) Ladd, J. N. *Soil Enzymes*; Burns, R. G., Ed. Academic Press: New York, 1978; pp 51−96.
(19) Herbert, R. B., Jr.; Benner, S. G.; Blowes, D. W. *Groundwater Quality: Remediation and Protection;* IAHS Publication no. 250; Tubingen, Germany, September 21−25, 1998; pp 451−458.
(20) Canfield, D. E.; Raiswell, R.; Westrich, J. T.; Reaves, C. M.; Berner, R. A. *Chem. Geol.* **1986**, *54*, 149−155.
(21) Allison, J. D.; Brown, D. S.; Nova-Gradac, K. J. *MINTEQA2/PRODEFA2, A geochemical assessment model for environmental systems: Version 3.0 user's manual.*; U.S. E.P.A.: Athens, GA, 1990.

(22) Ball, J. W.; Nordstrom, D. K. *User's manual for WATEQ4F, with revised thermodynamic database*; Open File Report 91-183; U.S. G.S.: 1991.
(23) Stumm, W.; Morgan, J. J. *Aquatic Chemistry*; John Wiley & Sons: New York, 1981; p 543.
(24) Chambers, L. A.; Trudinger, P. A. *Geomicrobiol. J.* **1979**, *1*, 249−293.
(25) Morse, J. W.; Millero, F. J.; Cornwell, J. C.; Rickard, D. *Earth Sci. Rev.* **1987**, *24*, 1−42.
(26) Boudreau, B. P.; Canfield, D. E. *Geochim. Cosmochim. Acta* **1993**, *57*, 317−334.
(27) Hiebert, F. K.; Bennett, P. C. *Science* **1992**, *258*, 278−281.
(28) Bennett, P. C. *Geochim. Cosmochim. Acta* **1991**, *55*, 1781−1897.
(29) Waybrant, K. R.; Blowes, D. W.; Ptacek, C. J. *Environ. Sci. Technol.* **1998**, *32*, 1972−1979.
(30) Baldi, F.; Pepi, M.; Burrini, D.; Kniewald, G.; Scali, D.; Lanciotti, E. *Appl. Environ. Microbiol.* **1996**, *62*(7), 2398−2404.
(31) Connell, W. E.; Patrick, W. H. *Science* **1968**, *159*, 86−87.

Received for review October 7, 1998. Revised manuscript received May 26, 1999. Accepted June 1, 1999.

ES981040U